Optimally Designed Quantum Transport across Disordered Networks

Mattia Walschaers,[1,2,*] Jorge Fernandez-de-Cossio Diaz,[3,†] Roberto Mulet,[1,3,‡] and Andreas Buchleitner[1,§]

[1]*Physikalisches Institut, Albert-Ludwigs-Universitat Freiburg, Hermann-Herder-Strasse 3, D-79104 Freiburg, Germany*
[2]*Instituut voor Theoretische Fysica, KU Leuven, Celestijnenlaan 200D, B-3001 Heverlee, Belgium*
[3]*Department of Theoretical Physics, Complex System Group, University of Havana, Ciudad de La Habana 10400, Cuba*

(Received 24 June 2013; published 29 October 2013)

We establish a general mechanism for highly efficient quantum transport through finite, disordered 3D networks. It relies on the interplay of disorder with centrosymmetry and a dominant doublet spectral structure and can be controlled by the proper tuning of *only* coarse-grained quantities. Photosynthetic light harvesting complexes are discussed as potential biological incarnations of this design principle.

DOI: 10.1103/PhysRevLett.111.180601 PACS numbers: 05.60.Gg, 03.65.Xp, 72.10.−d, 87.15.hj

In a variety of fields, ranging from quantum information [1] to solar cell physics [2], the efficient transport of quanta is of paramount importance. In realistic setups, however, one typically encounters systems which are complex in nature and only allow for a limited degree of control. Therefore, it is relevant to understand which general conditions are required to exploit fundamental principles of quantum mechanics to enhance transport in complex systems. At the present, this question is still widely open.

Common wisdom suggests that quantum interference can enhance transport across perfectly periodic potentials [3,4], while it tends to suppress transport in disordered systems [5,6]. In general, multipath quantum interference leads to erratic, large scale fluctuations of transmission probabilities when boundary conditions or other system parameters are slightly changed [7–11]. These fluctuations are often indicative of the strong, nonlinear coupling of few degrees of freedom, as it abounds in heavy nuclei [7], ultracold many-particle dynamics [12], strongly perturbed Rydberg systems [13–15], billiard geometries for photons [16] and electrons [17], strongly driven quantum systems [18], and in large molecules [19–21]. Often, devices which transport quanta tend to avoid these fluctuations; however, one may wonder whether they can be harvested.

Here, we seek to identify design principles for the properties of disordered Hamiltonians that, supported by large scale fluctuations, may generate *quantum-enhanced* transport. These design principles are statistically robust, in the sense that they are "implementable" by controlling only few coarse-grained parameters. We show that a collection of random Hamiltonians amended by only two additional constraints features high probabilities for rapid, near-to-perfect single-excitation transport across the abstract networks they can be associated with. The probability distributions of transfer times and efficiencies are fully controlled by the networks' electronic density of states, some *average* coupling matrix element, and the complex size (in terms of number of constituents), which are easily controllable, e.g., in macromolecular design [22–25]. As a potential application, we discuss the possible role of our findings for efficient light harvesting in photosynthetic complexes. While it is not our intention to perform a detailed analysis of these complex biological functional units, we rather wish to scrutinize the introduced design principles in the light of available structure data.

As a working model, we consider the coherent transport of one excitation across a disordered 3D network of N sites. Hilbert space is spanned by the basis states $|i\rangle$ which represent those states where the excitation is fully localized at the network's site i. In order to formulate a quantitative, statistical theory, we generate different realizations of disorder by sampling over $N \times N$ random Hamiltonians H extracted from the Gaussian orthogonal ensemble (GOE) [26]. The matrix entries $H_{i,j}$ encode the couplings between sites i and j. For each realization, input $|\text{in}\rangle$ and output $|\text{out}\rangle$ states are defined by those sites with the weakest coupling $V = \min_{i \neq j}|H_{i,j}|$, since we wish to understand the (ideally constructive) impact of the additional, intermediate sites of the network on the effective coupling between $|\text{in}\rangle$ and $|\text{out}\rangle$. Our figure of merit is the transfer efficiency

$$\mathcal{P}_H = \max_{t \in [0, T_R)} |\langle \text{out}, \phi(t)\rangle|^2, \quad |\phi(0)\rangle = |\text{in}\rangle, \tag{1}$$

which quantifies a given random network's performance in terms of excitation transport. $\mathcal{P}_H$ is gauged against the direct coupling V between $|\text{in}\rangle$ and $|\text{out}\rangle$, in the absence of all intermediate sites, through the definition of the associated benchmark time scale $T_R = \pi/2V$ [27,28] (with respect to which time and energy will be rescaled in all subsequent statistical analysis, when sampling over different realizations of H).

Earlier studies of coupled dipoles suggested that a *centrosymmetric* structure of the Hamiltonian with respect to $|\text{in}\rangle$ and $|\text{out}\rangle$ is a valuable ingredient for perfect-state transfer in dipole-dipole networks [29–31]. This symmetry is defined by $JH = HJ$ and $|\text{in}\rangle = J|\text{out}\rangle$ [32], where J is the exchange matrix $J_{i,j} = \delta_{i,N-j+1}$ [33]. However, for GOE Hamiltonians on which centrosymmetry is imposed, the transfer efficiencies are still rather broadly distributed, implying that centrosymmetry alone is not sufficient for efficient state transfer. We need to identify an additional structural element which guarantees robustness, in the

sense that the transfer efficiency must not depend strongly on the specific conformation of the intermediate sites. Such a feature is also of obvious relevance for our model's applicability to real light harvesting complexes, which continuously undergo conformational changes (whether noisy or deterministic) on the macromolecular scale.

Intuitively, the structural stability of efficient excitation transfer from $|\text{in}\rangle$ to $|\text{out}\rangle$ is guaranteed if both states are coupled through a *dominant tunneling doublet* [34]. The sole role of the intermediate states is then to *collectively amend* the effective tunneling coupling by an energy shift Δs. If Δs, which strongly fluctuates under variations of the network conformation (induced by the coupling to some background degrees of freedom, e.g., vibrational modes of macromolecular structures [35]), has the proper sign, this can lead to a *dramatic* enhancement of the transfer efficiency [36,37]. Such collective shifts induced by the coupling to random states have been investigated in the context of *chaos-assisted tunneling* [36,38–40] and will enter as the key ingredient of the subsequent analytical description of our problem.

Given the centrosymmetry of H, it can be cast, through an orthogonal transformation to the eigenbasis of J, into the block diagonal representation [33]

$$H = \begin{pmatrix} H^+ & 0 \\ 0 & H^- \end{pmatrix}. \tag{2}$$

In this new form, both H^+ and H^- are $N/2 \times N/2$ GOE matrices, i.e., the $H^{\pm}_{i,j}$ stem from a Gaussian distribution with zero mean and variance $(1 + \delta_{i,j})2\xi^2/N$.

Since two of the eigenvectors of J have the form $|\pm\rangle = (1/\sqrt{2})(|\text{in}\rangle \pm |\text{out}\rangle)$, we now additionally assume (see above) that $|+\rangle$ and $|-\rangle$ form a dominant doublet, close to eigenstates $|\tilde{+}\rangle$ and $|\tilde{-}\rangle$ of H^+ and H^-, respectively, [41]. It is then useful to write the Hamiltonian (2) as

$$H = \begin{pmatrix} E+V & \langle \mathcal{V}^+| & & \\ |\mathcal{V}^+\rangle & H^+_{\text{sub}} & & \\ & & E-V & \langle \mathcal{V}^-| \\ & & |\mathcal{V}^-\rangle & H^-_{\text{sub}} \end{pmatrix}, \tag{3}$$

which makes the definition of rows and columns which relate to $|+\rangle$ and $|-\rangle$ explicit. From the definition of $|\pm\rangle$, it is easy to see that $\langle \pm|H|\pm\rangle = E \pm V$. $|\mathcal{V}^{\pm}\rangle$ encodes the (Gaussian distributed) couplings of the dominant doublet states $|\pm\rangle$ to the remainder of the system.

Because of the dominant doublet assumption $|\langle \tilde{\pm}, \pm\rangle|^2 > \alpha \approx 1$, the norm $\|\mathcal{V}^{\pm}\|$ of the coupling is small and, under this condition, perturbation theory guarantees that $E \pm V$ in Eq. (3) are eigenvalues of H, up to some perturbative correction $s^{\pm}$. The explicit expression for the transfer efficiency is then dominated by those terms associated with $|\tilde{\pm}\rangle$, leading to the estimate

$$\mathcal{P}_H > \max_{t\in[0,T_R)} \frac{2\alpha - 1}{4} |e^{-it(E+V+s^+)} - e^{-it(E-V+s^-)}|^2, \tag{4}$$

where $s^{\pm} = \sum_i (|\langle \mathcal{V}^{\pm}, \psi_i^{\pm}\rangle|^2/E \pm V - e_i^{\pm})$ and $|\psi_i^{\pm}\rangle$ and $e_i^{\pm}$ are the eigenvectors and eigenvalues of $H^{\pm}_{\text{sub}}$. From Eq. (4), it is clear that the efficiency is large $\mathcal{P}_H > 2\alpha - 1$, if the first passage time [42] $t = \pi/|2V + \Delta s|$, $\Delta s = s^+ - s^-$, is smaller than T_R, with effective tunneling rate $|2V + \Delta s|$. All realizations with $T_R/t > 1$ exhibit efficient transport *faster* than the direct coupling between $|\text{in}\rangle$ and $|\text{out}\rangle$. Note that the dominant doublet assumption alone does not guarantee this latter feature; rather, it is a fundamental consequence of the strong fluctuations of Δs that arise due to the disorder inscribed into $\|\mathcal{V}^{\pm}\|$ and $H^{\pm}_{\text{sub}}$. This may be induced, for example, by the coupling of some complex background degrees of freedom, such as vibrational modes [35]. Only a sufficiently broad distribution of Δs guarantees that *fast* efficient transfer can always be achieved, even if the direct coupling between the input and output sites tends to zero [38]. Thus, despite being weakly coupled, the presence of the intermediate, random sites of the network represented by $H^{\pm}_{\text{sub}}$ is absolutely crucial to achieve efficient transport.

For fixed E and V, the distribution of Δs was shown to be a Cauchy distribution (for sufficiently large N) in Refs. [36,37,39]. In our present problem, E and V are themselves stochastic variables and, therefore, should be averaged over. Since the integrations over E and V are dominated by their mean values, given by $\bar{V} \approx 2\pi\sqrt{2}\xi e^{-1}N^{-3/2}$ and $\bar{E} = 0$, a lengthy but straightforward calculation shows that the probability distribution of $T_R(2V + \Delta s)/\pi = T_R/t$ is given by

$$P\left(\frac{T_R}{t} = x\right) = \frac{1}{\pi}\left(\frac{s_0}{s_0^2 + (1 + x_0 + x)^2} + \frac{s_0}{s_0^2 + (1 + x_0 - x)^2}\right), \tag{5}$$

with $s_0 = (\overline{\|\mathcal{V}\|^2} Ne(1 - 2/N)^{1/2}/4\pi\xi^2)$, $x_0 = (\overline{\|\mathcal{V}\|^2}/2\xi^2)$, and $\overline{\|\mathcal{V}\|^2}$ the expectation value of $\|\mathcal{V}^{\pm}\|^2$ for all realizations where the dominant doublet assumption holds.

The distribution (5) depends on only two *coarse-grained* parameters: ξ characterizes the spectral density of the eigenstates of H^+_{sub} and H^-_{sub}, while $\overline{\|\mathcal{V}\|^2}$ measures the average coupling strength of the dominant doublet to these states. It therefore cannot be emphasized enough that, within the picture here elaborated, the transport properties of the problem *do not* depend on the specificities of the Hamiltonian or on the intermediate electronic states of the network.

To validate our theoretical model by numerical simulations, we generate many GOE Hamiltonians with the additional constraint of centrosymmetry with respect to $|\text{in}\rangle$ and $|\text{out}\rangle$. For each of these Hamiltonians, the existence of a dominant doublet is assessed by inspection of its eigenvectors and by verifying that, for some $|\tilde{\pm}\rangle$, the condition $|\langle \tilde{\pm}, \pm\rangle|^2 > \alpha$ holds. This postselection defines the statistical ensemble which we expect to satisfy (5). $\mathcal{P}_H$ is then obtained by numerical propagation of the quantum dynamics generated by the Hamiltonian, by virtue of Eq. (1). The

associated transfer time is extracted in two independent ways, due to the following subtlety: A random Hamiltonian of type (3) will generate quasiperiodic dynamics, such that subsequent maxima of $|\langle \text{out}, \phi(t)\rangle|^2$ may slightly differ in magnitude. Direct propagation of $|\phi(0)\rangle$ can therefore result in values of $\mathcal{P}_H$ slightly larger than the lower bound of Eq. (4), if T_R accommodates more than one maximum of $|\langle \text{out}, \phi(t)\rangle|^2$. This will happen at larger values of t; hence, larger values of x will be suppressed. The strong fluctuations of the dashed line in Fig. 1 are an expression thereof. An alternative way to extract t is by direct inspection of the spectrum and by using the fact that $T_R/t = |2V + \Delta s|/|2V|$ [see Eq. (4)]. This method is immune against tiny corrections to the bound (4) and yields perfect agreement with Eq. (5), as shown in Fig. 1.

No free parameters are involved in this plot: The values $\xi = 2$, $\alpha = 0.95$, and $\overline{\|\mathcal{V}\|^2} = 0.311\,962$ which enter Eq. (5) are either given *a priori* or extracted from the statistics of the numerically generated sample Hamiltonians. Clearly, the majority of realizations has t smaller than the time scale set by the direct coupling V between $|\text{in}\rangle$ and $|\text{out}\rangle$. The fat algebraic tail of the Cauchy distribution for $t \ll T_R$ guarantees that realizations with very fast transport are abundant in the sense that they are not exponentially unlikely.

For fixed $\alpha = 0.95$, our model predicts efficiencies larger than $\mathcal{P}_H > 2\alpha - 1 = 0.9$. This is indeed observed in the simulations. The inset in Fig. 1 shows the probability density of the transfer efficiency, which is sharply peaked above $\mathcal{P}_H > 0.9$ (indicated by the arrow). Comparison, in the same figure, with the efficiency distributions for centrosymmetric GOE matrices without the doublet constraint and for general GOE matrices, respectively, shows that in both cases, the average efficiency is significantly lower than for those centrosymmetric Hamiltonians which exhibit the additional design element of a dominant doublet.

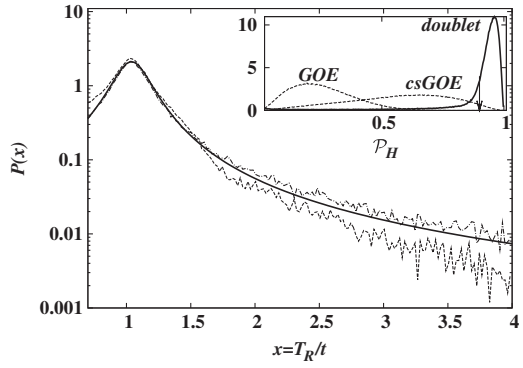

FIG. 1. Comparison of the numerically inferred distributions of inverse transfer times T_R/t (dashed and dash-dotted lines) to the prediction (5) (solid line) for density of states $\xi = 2$, $N = 10$ network sites, with the dominant doublet condition $\alpha = 0.95$. $\overline{\|\mathcal{V}\|^2} = 0.311\,962$ is extracted from the numerical sample. The dashed line is derived from numerical propagation of the initial state $|\phi(0)\rangle$ in the time window $[0, 1.7T_R]$, via Eq. (1), while the dash-dotted line is inferred from the spectrum of the Hamiltonian, via $T_R/t = |2V + \Delta s|/|2V|$ [see Eq. (4)]. Inset: Histograms of the transfer efficiencies $\mathcal{P}_H$ for three different ensembles ξ and N as above. Constraining the ensemble from GOE to centrosymmetric and to centrosymmetric with the dominant doublet condition $\alpha = 0.95$ dramatically enhances the average efficiencies.

A remarkable asset of this transport mechanism is its robustness under different realizations of disorder, which, in the context of networks, refers to different configurations of the intermediate sites [represented by the random matrices $H^{\pm}_{\text{sub}}$ in Eq. (3)]. In the light of the recent debate on the potential role and unexpected robustness of quantum coherence in photosynthetic harvesting of the sunlight's energy [35], one may wonder whether the proposed design principles are implemented by nature. Indeed, some of the light harvesting complexes which are hardwired in bacteria or plants, such as the Fenna-Matthews-Olson (FMO) complex of green sulfur bacteria [43–45], exhibit an apparently disordered, networklike structure and appear to be optimized for efficient transport.

It is therefore suggestive to test the hypothesis that centrosymmetry and the dominant doublet are compatible with the available structure data [43,44]. For this purpose, we fix the spatial position of the FMO's constituent bacteriochlorophyll-a (BChla) molecules as given in the literature [43] (see Table I of the Supplemental Material [46]) and only allow the orientation of the dipoles associated with each BChla to vary. Furthermore, we neglect on-site energy shifts induced by the coupling to background degrees of freedom; i.e., all on-site energies are assumed to be identical. Apart from a possible limitation of the maximally achievable transfer efficiencies to values smaller than 100% (similar to the limitation of the maximum transfer amplitude by the bias in an asymmetric double-well potential), this does not affect the central features of our transport scenario [31].

Given the spatial positions of the dipoles, the intersite dipole-dipole coupling matrix elements $H_{i,j}$ are determined by their relative orientations [44] (see Table II of the Supplemental Material [46]). To certify the relevance of our dominant doublet picture, we now ask the question of how close the documented FMO conformations are to optimal conformations in the above sense. To give an answer to this question, we use the tabulated FMO data to seed a genetic algorithm with the transfer efficiency (1) as a target function and only allow for variations of the intermediate sites' dipole orientations (variations of the coupling to and between the intermediate sites generate the nontrivial and crucial statistics of the level shifts Δs in the underlying chaos-assisted tunneling scenario). We then correlate the thus achieved optimal transfer efficiencies with the optimal networks' centrosymmetry quantifiers [31] $\epsilon = (1/N)\min_S \|H - J^{-1}HJ\|$ (where the minimization runs over all permutations of the intermediate network sites $2, \ldots, N-1$, and the Hilbert-Schmidt norm [47] is employed) and the dominant

doublet strengths α (defined as the minimum of $|\langle \tilde{\mp}, + \rangle|^2$ and $|\langle \tilde{-}, - \rangle|^2$). These results are benchmarked against optimization results seeded by random orientations of the dipoles and illustrated in Fig. 2. Filled blue circles represent the results delivered by the genetic algorithm when launched in the vicinity of the documented FMO structure—which itself exhibits (poor) efficiency, doublet strength, and centrosymmetry as represented by the red filled circles in both plots. The synchronous trend towards significantly enhanced efficiencies, centrosymmetries, and doublet strengths is *unambiguous and in stark contrast* to the benchmark ensemble represented by crosses in the plot, which also reflects some correlation between efficiency, centrosymmetry, and doublet strength, but lacks the essentially deterministic attraction towards optimal performance which manifests in the FMO's vicinity.

On top of this evolutionary attraction towards optimal performance in the FMO neighborhood, in response to our above question, the dipole orientations which result from evolutionary optimization are indeed very close to the dipole orientations as given by the experimental data: Fig. 3 depicts the probability densities for the relative positions of the *optimal* dipole orientations at each of the intermediate BChla sites, in (ϕ, θ) spherical coordinates with respect to the tabulated orientations which define the origin of each plot. In the worst case, the average orientation of dipole 4 deviates by less than 20% from the experimental data. All the other optimized dipole orientations deviate by less than 7%. Therefore, the documented FMO dipole structure has a design that is close to optimal with respect to the abstract design principles which we introduced above.

In summary, we described a general mechanism that gives rise to fast and near-to-perfect quantum transport in finite, 3D disordered systems. The mechanism rests on two crucial design principles: The *centrosymmetry* of the underlying Hamiltonian, which guarantees a natural block diagonal representation, and the existence of a *dominant doublet* that ensures that the coupling to random states (provided, e.g., by the intermediate sites of a molecular network) can efficiently assist the transport in a robust way. The statistics of the transfer efficiencies and times, as shown in Fig. 1, then only depend on the intermediate network sites' density of states ξ and on the average coupling strength $\overline{\|\mathcal{V}\|^2}$ of the in- and output sites to the network. While the former can be controlled, e.g., by the packing of the intermediate network sites, the latter should be easily controllable by fixing—e.g., through a protein scaffold [48]—their average distance to the input and output. Within this perspective, robust and efficient transport across complex quantum networks may be achieved by optimally designing *not* one single network conformation but rather a *suitable statistical distribution*, fixed by the density of states and some average coupling strength alone.

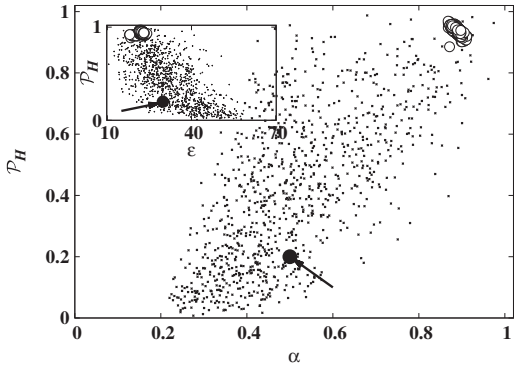

FIG. 2. Scatter plots of transfer efficiency $\mathcal{P}_H$ versus dominant doublet strength α and centrosymmetry ϵ (inset). Evolutionary optimization as achieved by a genetic algorithm is indicated by the empty circles, upon the seeding of the algorithm with the documented FMO structure (indicated by an arrow and a black circle and listed in Tables I and II of the Supplemental Material [43,44,46]). The unambiguous and synchronous attraction towards more efficient, centrosymmetric dipole orientations with large doublet strengths is to be compared to a benchmark ensemble generated by the algorithm when seeded with randomized dipole orientations (dots).

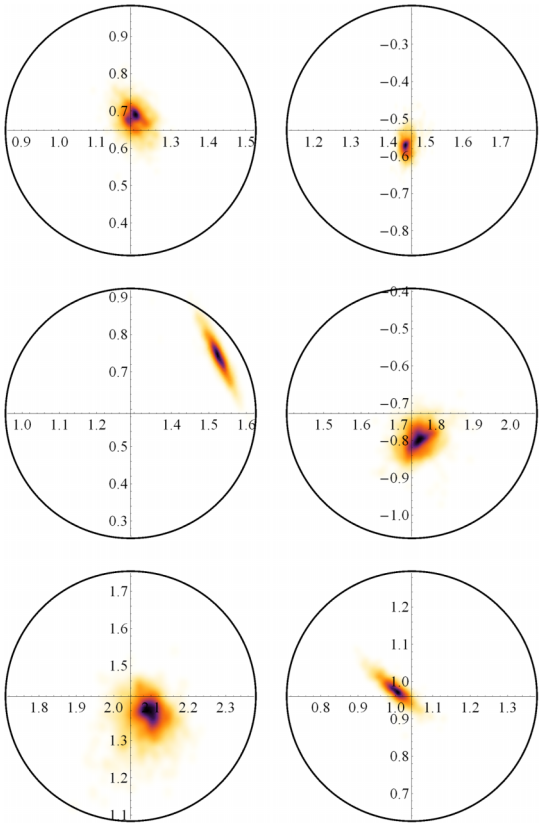

FIG. 3 (color online). (Linearly) gray scaled probability density of the genetically optimized FMO dipole orientations, in spherical coordinates (ϕ, θ) (in radian). Dipoles 1, 2, 4, 5, 6, and 7 are listed from left to right and top to bottom, and the experimental dipole orientation extracted from Table II (of the Supplemental Material [46]) defines the origin of each plot. Dipoles 8 (input) and 3 (output) are not shown, since we keep their orientations fixed during optimization.

R. M. acknowledges support by the Alexander von Humboldt Stiftung. M. W. and A. B. are grateful for funding within the DFG Research Unit 760 and for support through the EU COST Action MP1006. M. W. acknowledges partial funding by the Belgian Interuniversity Attraction Poles Programme P6/02 and FWO Vlaanderen Project No. G040710N, and by the German National Academic Foundation.

*mattia@itf.fys.kuleuven.be
†jfernandez@estudiantes.fisica.uh.cu
‡roberto.mulet@gmail.com
§abu@uni-freiburg.de

[1] D. Burgarth and S. Bose, New J. Phys. **7**, 135 (2005).
[2] J. Nelson, *The Physics of Solar Cells* (Imperial College Press, London, 2010).
[3] N. W. Ashcroft and N. D. Mermin, *Solids State Physics* (Saunders College Publishing, Philadelphia, 1976).
[4] Y. Aharonov, L. Davidovich, and N. Zagury, Phys. Rev. A **48**, 1687 (1993).
[5] P. W. Anderson, Phys. Rev. **109**, 1492 (1958).
[6] G. Modugno, Rep. Prog. Phys. **73**, 102401 (2010).
[7] G. E. Mitchell, A. Richter, and H. A. Weidenmüller, Rev. Mod. Phys. **82**, 2845 (2010).
[8] B. Kramer and A. MacKinnon, Rep. Prog. Phys. **56**, 1469 (1993).
[9] J. Madroñero, A. Ponomarev, A. R. R. Carvalho, S. Wimberger, C. Viviescas, A. Kolovsky, K. Hornberger, P. Schlagheck, A. Krug, and A. Buchleitner, Adv. At. Mol. Opt. Phys. **53**, 33 (2006).
[10] *Quantum Transport and Dissipation*, edited by T. Dittrich, P. Hänggi, G. L. Ingold, B. Kramer, G. Schön, and W. Zwerger (Wiley-VCH, Weinheim, 1998).
[11] S. Löck, A. Bäcker, R. Ketzmerick, and P. Schlagheck, Phys. Rev. Lett. **104**, 114101 (2010).
[12] A. Rodriguez, A. Chakrabarti, and R. A. Römer, Phys. Rev. B **86**, 085119 (2012).
[13] N. N. Choi, M. H. Lee, and G. Tanner, Phys. Rev. Lett. **93**, 054302 (2004).
[14] J. Madroñero and A. Buchleitner, Phys. Rev. Lett. **95**, 263601 (2005).
[15] J. H. Gurian, P. Cheinet, P. Huillery, A. Fioretti, J. Zhao, P. L. Gould, D. Comparat, and P. Pillet, Phys. Rev. Lett. **108**, 023005 (2012).
[16] H.-J. Stöckmann and J. Stein, Phys. Rev. Lett. **64**, 2215 (1990).
[17] A. S. Sachrajda, R. Ketzmerick, C. Gould, Y. Feng, P. J. Kelly, A. Delage, and Z. Wasilewski, Phys. Rev. Lett. **80**, 1948 (1998).
[18] A. R. R. Carvalho and A. Buchleitner, Phys. Rev. Lett. **93**, 204101 (2004).
[19] S. Keshavamurthy and P. Schlagheck, *Dynamical Tunneling—Theory and Experiment* (CRC Press, Boca Raton, FL, 2011).
[20] J. Baier, M. Gabrielsen, S. Oellerich, H. Michel, M. van Heel, R. J. Cogdell, and J. Köhler, Biophys. J. **97**, 2604 (2009).
[21] T. P. J. Krüger, E. Wientjes, R. Croce, and R. van Grondelle, Proc. Natl. Acad. Sci. U.S.A. **108**, 13 516 (2011).
[22] M. Kozaki, A. Uetomo, S. Suzuki, and K. Okada, Org. Lett. **10**, 4477 (2008).
[23] M. R. Wasielewski, Acc. Chem. Res. **42**, 1910 (2009).
[24] M. Kozaki, K. Akita, K. Okada, D.-M. S. Islam, and O. Ito, Bull. Chem. Soc. Jpn. **83**, 1223 (2010).
[25] S. Gerlich, S. Eibenberger, M. Tomandl, S. Nimmrichter, K. Hornberger, P. J. Fagan, J. Tüxen, M. Mayor, and M. Arndt, Nat. Commun. **2**, 263 (2011).
[26] M. L. Mehta, *Random Matrices* (Elsevier, Amsterdam, 2004).
[27] T. Scholak, F. Mintert, T. Wellens, and A. Buchleitner, Semicond. Semimet. **83**, 1 (2010).
[28] T. Scholak, T. Wellens, and A. Buchleitner, Europhys. Lett. **96**, 10 001 (2011).
[29] M. Christandl, N. Datta, T. C. Dorlas, A. Ekert, A. Kay, and A. J. Landahl, Phys. Rev. A **71**, 032312 (2005).
[30] A. Kay, Phys. Rev. A **73**, 032306 (2006).
[31] T. Zech, R. Mulet, T. Wellens, and A. Buchleitner, arXiv:1205.5519; T. Zech, M. Walschaers, T. Scholak, R. Mulet, T. Wellens, and A. Buchleitner, Fluct. Noise Lett. **12**, 1340007 (2013).
[32] This constraint actually implies that $V = \min_i |H_{i,N-i+1}|$.
[33] A. Cantoni and P. Butler, Linear Algebra Appl. **13**, 275 (1976).
[34] A. Wójcik, T. Łuczak, P. Kurzyński, A. Grudka, T. Gdala, and M. Bednarska, Phys. Rev. A **75**, 022330 (2007).
[35] T. Mančal, N. Christensson, V. Lukeš, F. Milota, O. Bixner, H. F. Kauffmann, and J. Hauer, J. Chem. Phys. Lett. **3**, 1497 (2012).
[36] F. Leyvraz and D. Ullmo, J. Phys. A **29**, 2529 (1996).
[37] G. Ergün and Y. V. Fyodorov, Phys. Rev. E **68**, 046124 (2003).
[38] S. Tomsovic and D. Ullmo, Phys. Rev. E **50**, 145 (1994).
[39] J. Zakrzewski, D. Delande, and A. Buchleitner, Phys. Rev. E **57**, 1458 (1998).
[40] W. K. Hensinger, H. Häffner, A. Broawaeys, N. R. Heckenberg, K. Helmerson, C. McKenzie, G. J. Milburn, W. D. Philips, S. L. Rolston, H. Rubinsztein-Dunlop, and B. Upcroft, Nature (London) **412**, 52 (2001).
[41] Note that the dominant doublet assumption is much more natural [38] given centrosymmetry than in its absence: While in the former case, the dominant doublet is an element of the natural basis given by the eigenstates of J, it is an *ad hoc* assumption without such discrete symmetry of the underlying Hamiltonian. Accordingly, it can be shown that the probability density of dominant doublets without centrosymmetry is quadratically suppressed as compared to the centrosymmetric case.
[42] T. Okubo and T. Odagaki, Phys. Rev. E **73**, 026128 (2006).
[43] D. E. Tronrud, J. Wen, L. Gay, and R. E. Blankenship, Photosynth. Res. **100**, 79 (2009).
[44] M. Schmidt am Busch, F. Müh, M. E. Madjet, and T. Renger, J. Phys. Chem. Lett. **2**, 93 (2011).
[45] G. D. Scholes, T. Mirkovic, D. B. Turner, F. Fassioli, and A. Buchleitner, Energy Environ. Sci. **5**, 9374 (2012).
[46] See Supplemental Material at http://link.aps.org/supplemental/10.1103/PhysRevLett.111.180601 for an overview of the structural data for the FMO complex and for the details of the genetic algorithm which was used to study these data.
[47] M. Reed and B. Simon, *Methods of Modern Mathematical Physics* (Academic, New York, 1981), 1st ed., Vol. 1.
[48] G. D. Scholes, G. R. Fleming, A. Olaya-Castro, and R. van Grondelle, Nat. Chem. **3**, 763 (2011).